Type-2 Neuro Fuzzy Current Controlled Inverter Fed Induction Motor Drive

R. Ramanjan Prasad, G. Durga Sukumar

***Abstract-** As the conventional PI controller's operation is not satisfactory due to the operating point oscillations in a closed loop system, intelligent based controllers are employed. This paper presents Neuro Type 2 fuzzy controlled (NT2FC) based speed controller in the IVC of induction motor. The advantage of T2NFC is the area of point of intersection of membership functions is less so the value obtained by the centroid method is more accurate compared to NT1FC system. This paper presents performance comparison of IVC of IMD with conventional PI, NT1FC and NT2FC. The tuning of type 2 fuzzy membership functions is done using neural network by applying LSE in forward pass and BP algorithm in backward pass. The experimental validation is also carried out using Dspace 1104 micro controller. The date of at this experimental validation has been taken from the simulation. It is carried out considering 2HP Induction motor and it is observed that the NT2FC gives better performance of IMD.*

***Index Terms-** Neuro Type-2 fuzzy controller (NT2FC), Neuro Type-1 fuzzy controller (NT1FC), Space vector modulation (SVM), Induction motor drive (IMD), Proportional and integral controller (PI) and Indirect Vector Control (IVC).*

I. INTRODUCTION

For the better performance of the IM, field-oriented control method is widely used. By using Parks & inverse Parks transformation, the phase angle and amplitude of the induction motor flux and current are decoupled. The indirect and direct field -oriented control techniques are two categories in vector control method based on what way the field angle is obtained. The unit vectors in the vector control obtained based on the mathematical modeling of induction motor [1-3]. The indirect vector is widely used in industrial controlled drives due to elimination of flux sensor in the system, but it requires position sensor of rotor [3,4]. Induction motor controllers are conventionally proportional and integral (PI) and PID controllers. The model is very uncertain because of its parameter variations such as temperature changes, saturation and system disturbances in the system. The drawbacks of the above problems due to modelling can be overcome by using soft computing-based controllers are employed in the field control to enhance the performance [5-6]. For Multilevel inverter the most promising method is Space Vector Modulation (SVM) when comparison is made with different techniques, because it gives enormous adaptability to maintain switching frequency as constant. To observe better output voltage for AC drives different SVM algorithms are employed for multilevel inverters.

Revised Manuscript Received on November 15, 2019

R.RamanjanPrasad, VFSTR University, Vadlamudi, Guntur,
G.Durga Sukumar, VITS, Deshmukhi, Nalgonda

Space vector modulation is implemented by properly choosing and performing switching conditions of the carrier wave used on corresponding on times. According to the inverter levels, the number of triangles increases which increases the difficulty of Space Vector Modulation for multilevel inverters [7-8]. Performance of IM using NF based SVM technique is compared with conventional SVM for various parameters like current, speed and torque [9]. A diode-clamped three-level inverter (TDCI) with PI and type 2 controllers in the DTC of induction motor (IM) with space vector modulation has been presented [11-12]. The comparative performance of type I and type II FLC's of induction motor torque and flux has been presented [13]. The induction motor performance using ANFIS based controllers has been presented [14]. The performance of the PI and T1NFC in the indirect vector control fed induction motor are compared with T2NFC and improvement of the performance of the drive system is obtained.

This paper organized in six sections, in this, Mathematical modelling of induction motor is introduced in the second section. The third section presents the IVC scheme of IM. The proposed type 2 neuro fuzzy based indirect vector-controlled IMD is presented in fourth section. The forward and backward pass algorithm is presented in fifth section. The simulation results of type 2 neuro fuzzy and PI controller is presented in the sixth section. Experimental results presented in seventh section.

II. INDUCTION MOTOR MATHEMATHICAL MODELLING

The induction motor mathematical model with an arbitrary frame rotating at ω_r speed is expressed as follows:

Voltage equations

$$V_{QS} = R_S . i_{QS} + L_{QS} \frac{d}{dt} i_{QS} + M_Q . \frac{d}{dt} i_{QR} \tag{1}$$

$$V_{DS} = R_S . i_{DS} + \frac{d\lambda_{DS}}{dt} \tag{2}$$

$$V_{QR} = R_R i_{QR} + P\lambda_{QR} + e_{QR} \tag{3}$$

$$V_{DR} = R_{R.} i_{DR} + P\lambda_{DR} - (\omega_S - \omega_R) . \lambda_{QR} \tag{4}$$

$$V_{QS}(S) = (R_S + L_S . s) i_{QS} + \omega_S . i_{QS} + i_{QR} . L_M . s + \omega_S . L_M . i_{DR} \tag{5}$$

$$V_{DS(}(S) = R_S i_{DS} + p(l_S i_{DS} + l_M i_{DR}) + \omega_S (L_S i_{QS} + l_M i_{QR}) \tag{6}$$

$$V_{DS}(s) = i_{QS}(-\omega_S . l_S) + (R_s + l_s . s) i_{DS} - \omega_S (L_M . i_{QR} + L_M . s . i_{DR})$$
(7)

$$V_{QR} = R_R i_{QR} + \frac{d}{dt}(L_R . i_{QR} + L_M . i_{QS}) + (\omega_S - \omega_R)(L_R . i_{DR} + L_M \, i_{DS}) \quad (8)$$

$$V_{QR}(s) = i_{QS}[L_M . s] + i_{DS}[(\omega_S - \omega_R) L_M] + i_{QR}[R_R + L_R . s] + i_{DR}[(\omega_S - \omega_R) L_R] \quad \textbf{(9)}$$

$$\begin{bmatrix} V_{QS} \\ V_{DS} \\ V_{QR} \\ V_{DR} \end{bmatrix} = \begin{bmatrix} R_S + s.L_S & \omega_S L_S & L_M . s & \omega_S . L_M \\ -\omega_S . L_S & R_S + sL_S & -\omega_S . L_M & L_m . s \\ L_M . s & (\omega_S - \omega_R) L_M & R_R + s.L_R & (\omega_S - \omega_R) L_R \\ -(\omega_S - \omega_R) L_M & L_M . s & -(\omega_S - \omega_R) L_R & R_R + L_R . s \end{bmatrix} \begin{bmatrix} i_{QS} \\ i_{DS} \\ i_{QR} \\ i_{DR} \end{bmatrix} \quad \textbf{(10)}$$

For steady state s = zero

$$\begin{bmatrix} V_{QS} \\ V_{DS} \\ V_{QR} \\ V_{DR} \end{bmatrix} = \begin{bmatrix} R_S & \omega_S L_S & 0 & \omega_S . L_M \\ -\omega_S . L_S & R_S & -\omega_S . L_M & 0 \\ 0 & (\omega_S - \omega_R) L_M & R_R & (\omega_S - \omega_R) L_R \\ -(\omega_S - \omega_R) L_M & 0 & -(\omega_S - \omega_R) L_R & R_R + L_R . s \end{bmatrix} \begin{bmatrix} i_{QS} \\ i_{DS} \\ i_{QR} \\ i_{DR} \end{bmatrix} \quad (11)$$

Torque exerted by the motor

$$T_e = 3 \frac{p}{2} \frac{I_R^2 R_R}{s . \omega_S} \quad (12)$$

$$T_e = \frac{p}{2} \frac{P_g}{\omega_S} \quad (13)$$

$$P_g = 3 . V_m . I_R' . \omega_S (V_m . I_R') \quad (14)$$

$$T_e = \frac{p}{2} 3 \lambda_m I_R' . \mathrm{Sin}\,\theta \quad (15)$$

$$T_e = \frac{3p}{2}[\lambda_{DR} i_{QS} - i_{DS} \lambda_{QR}] \quad (16)$$

$$T_e = 3 \frac{p}{2}[\lambda_{DS} i_{QR} - \lambda_{QS} i_{DR}] \quad (17)$$

III. INDIRECT VECTOR CONTROL

The IVC is similar to that of DFOC apart from the unit vectors are obtained in an indirect manner. The IVC technique phasor diagram as shown in figure 1.

The d^e-q^e axes are rotating leading the axes of $D_R - Q_R$ at an angle θ_{sl} with respective to the slip frequency.

$$\theta_e = \int \omega_e dt = \int (\omega_e + \omega_{sl}) dt = \theta_R + \theta_{sl} \quad (18)$$

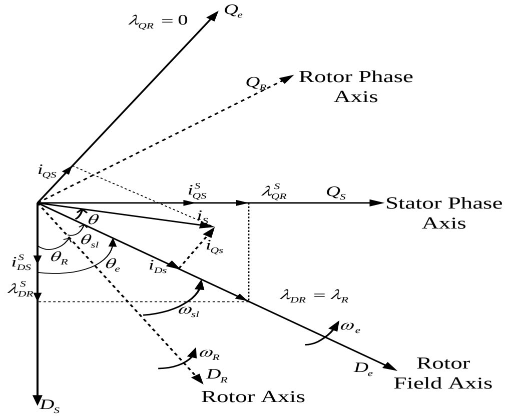

Figure 1. Phasor diagram of Indirect Vector Control

The equations rotor side are

$$\mathrm{P}\lambda_{DR} + \lambda_{DR} \frac{R_R}{L_R} - R_R i_{DS} \frac{L_M}{L_R} - \lambda_{QR} \omega_{sl} = 0$$
$$\mathrm{P}\lambda_{QR} + \lambda_{QR} \frac{R_R}{R_R} - R_R i_{QS} \frac{L_M}{L_R} + \lambda_{DR} \omega_{Sl} = 0 \quad (19)$$

For decoupling control, $\Psi_{qr} = 0$, $\mathrm{P}\Psi_{dr} = 0$, thus the flux of rotor Ψ_R is fixed on the D_e axis.

By using the above parameters

$$\frac{L_R}{R_R} \mathrm{P}\lambda_R + \lambda_R = L_M i_{DS} \quad (20)$$

The calculation of slip frequency as

$$\omega_{Sl} = \frac{L_M R_R}{\lambda_R L_R} i_{QS} \quad (21)$$

The Indirect Vector Control block diagram to estimate rotor angle θ_e as shown in Figure 2.

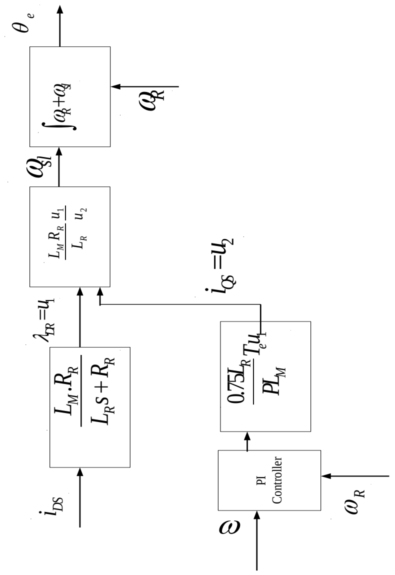

Fig 2. Rotor angle estimation of Indirect Vector Control

IV. IVC OF IMD USING T2NFC

T2NFCs are widely known to opponent to changes in parameters and noise which is suitable to cope with uncertainties of induction motor ad load variations.

The T2NFC architecture design combines learning algorithm with a seven-level neural network architecture and fuzzy logic and as shown in fig 3. The error in speed and changes of speed in error are the two inputs of the T2NFC, where ω_r^* is the command speed.

$$input^1 = e_\omega = \omega_r^* - \omega_r \quad (22)$$

$$input^2 = \Delta e_\omega = e_\omega(k) - e_\omega(k-1) \quad (23)$$

From the T-S fuzzy model, the two inputs error & change in error and outputs $y_1, y_2, \ldots, y_n$ can be given in generalized form as

Rule j (j=1,2--): if e_ω is m_j AND Δe_ω *is* n_j then

$$y_j \; is \; \sum_{j=1}^{A} m_j e_w + n_j \Delta e_w + r_j$$

where m_j and n_j are antecedent fuzzy. Here y_i is the output membership function.

Layer I: Input layer consists node member ship functions

$o_j^{\,1} = A_{mj}(e_\omega)$, j=1,2-----(24)

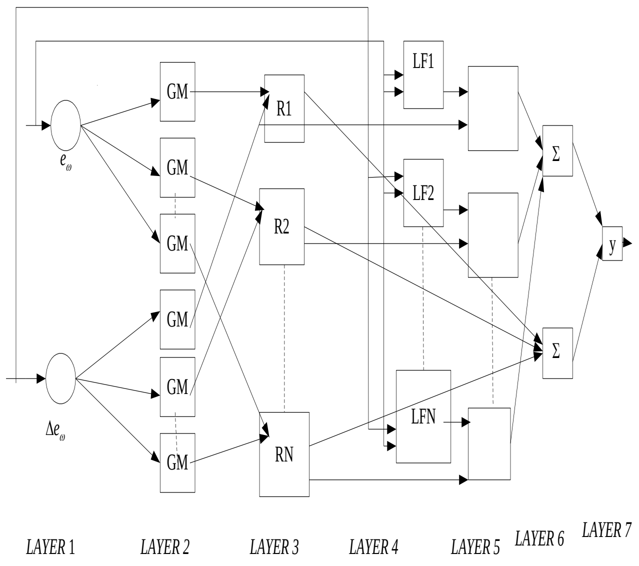

Figure 3. Architecture of NT2FC

$o_j^{\,1} = A_{nj}(\Delta e_\omega)$ j=1,…… (25)

Where A_{mj1} and A_{mj2} are gaussian membership functions. The mathematical equation is expressed as

$$A_{mj} = e^{\left(-0.5\left(\frac{(m_j - x)^2}{\sigma^2}\right)\right)}$$

$$A_{nj} = e^{\left(-0.5\left(\frac{(n_j - x)^2}{\sigma^2}\right)\right)} \qquad (26)$$

where x represents the Centre and σ represents the width of gaussian membership functions

Layer 2: Firing layer: Here output node calculates the firing strength of a rule

$$o_j^{\,2} = w_i = A_{mj}(e_\omega).A_{nj}(\Delta e_\omega)$$
$$= \min\left(A_{mj}(e_\omega), A_{nj}(\Delta e_\omega)\right), \; j = 1,2.....7 \qquad (27)$$

Layer 3: In this layer each node calculates the weight, which is normalized Firing strength

$$o_j^{\,3} = \overline{w_j} = \frac{w_j}{w_1 + w_2}, \; j = 1,2 \qquad (28)$$

Layer 4: Layer 4 is a De fuzzification layer, in this every node with a node function is given by

$$y_j \; is \; \sum_{j=1}^{A} m_j e_w + n_j \Delta e_w + r_j \qquad (29)$$

Where $\overline{w_j}$ is the output layer of 3 and m_{1j} is the parameter set.

Layer 5: It has only one node that produces the complete output that has the weighted sum of all combined outputs of the preceding layers and hence termed as an Output layer. Then the final output is given a

$$o_j^{\,5} = \frac{\sum w_j u_j}{\sum w_j}, \; j = 1,2.....7 \qquad (30)$$

V. LEARNING ALGORITHM

The amalgamation of mean Least squares optimization (LSE) and Gradient Descent Back Propagation algorithms give Least Squares optimization (LSE) and Gradient Descent Back Propagation algorithms gives rise as well as tuning to the fuzzy model. An error measure is reduced by adding the square of the difference among actual and desired output. Obtaining of error rate or the pre-determined epoch number prevents the training. The non-linear premise parameters are fine-tuned by implementing the gradient descent algorithm, on the other hand to minimize the linear consequent parameters the mean least-square is used.

Forward Pass as well as Backward Pass is composed in the learning algorithm at each period

Forward Pass

In the forward pass, each node output is calculated in T2NFC by training set of input patterns error(e_w) and change in error (Δe_ω) and Least Square estimator is used to categorize the rule consequent parameters. The duty ratio or output vector is a linear function in the Takagi-sugeno model. The Gaussian membership function enriched with three parameters a, b, & c, training set of 10000 inputs i.e. error and change in error & output duty ratio patterns are linear equations $(m_{1j}, n_{j,} \; and \; r_i)$ as

$$D_{1-N} = \overline{\omega_1}(1) f_1(1) + \overline{\omega_1} \; f_2(1) + ... + \overline{\omega_1} \; f_n(1)$$
$$D_{1-N} = \overline{\omega_1}(2) \; f_1(2) + \overline{\omega_1}(2) \; f_2(2) + ... + \overline{\omega_n}(2) f_n(2)$$

.

.

.

$$D_{1-N} = \overline{\omega_1}(N) f_1(N) + \overline{\omega_1}(N) f_2(N) + ...\overline{\omega_1}(N) f_n(N) \qquad (31)$$

$$D_1(1) = \overline{\omega_1}(1)[m_1 e_w(1) + n_1 \Delta e_w(1) + r_1]$$
$$\overline{\omega_2}(1)[m_2 e_w(1) + n_2 \Delta e_w(1) + r_2] + ... +$$
$$\overline{\omega_n}(1)[m_n e_w(1) + n_n \Delta e_w(1) + r_n]$$
$$D_1(2) = \overline{\omega_1}(2)[m_1 e_w(2) + n_1 \Delta e_w(2) + r_1] \qquad (32)$$
$$\overline{\omega_2}(2)[m_2 e_w(2) + n_2 \Delta e_w(2) + r_2] + ... +$$
$$= \overline{\omega_n}(2)[p_n e_w(2) + q_n \Delta e_w(2) + r_n]$$

.

.

Published By:
Blue Eyes Intelligence Engineering
& Sciences Publication

$$D_1(N)=\overline{\omega_1}(N)[m_1 e_w(N)+n_1\Delta e_w(N)+r_1]$$
$$\overline{\omega_2}(N)[m_2 e_w(N)+n_2\Delta e_w(N)+r_2]+.....+$$
$$\varpi_n(N)[m_n e_w(N)+n_n\Delta e_w(N)+r_n]$$

where N represents the input-output patterns, In the rule layer (= 25) n represents number of nodes, D_{1-N} is the expected duty ratio of the T2NFC.

The Eq. (32) represented as follows

$$D_{1-N} = AY, \quad (33)$$

where D_{1-N} is an $m \times 1 = 10{,}000 \times 1$

$$D_{1-N} = \begin{bmatrix} D_{1-N(1)} \\ D_{1-n(2)} \\ . \\ . \\ D_{1-N(N)} \end{bmatrix} \quad (34)$$

A can be represented by $M\ x\ X$ (1+number of inputs parameters=10,000x75 matrix,

$$A=\begin{bmatrix} \overline{\omega_1}(1) & \overline{\omega_1}(1)e_w(1) & \overline{\omega_1}(1)\Delta e_w(1) & . & . & \overline{\omega_n}(1) & \overline{\omega_n}(1)e_w(1) & \overline{\omega_n}(1)\Delta e_w(1) \\ \overline{\omega_1}(2) & \overline{\omega_1}(2)e_w(2) & \overline{\omega_1}(2)\Delta e_w(2) & . & . & \overline{\omega_n}(2) & \overline{\omega_n}(2)e_w(2) & \overline{\omega_n}(2)\Delta e_w(2) \\ . & . & . & . & . & . & . & . \\ . & . & . & . & . & . & . & . \\ \overline{\omega_1}(N) & \overline{\omega_1}(N)e_w(N) & \overline{\omega_1}(N)\Delta e_w(N) & . & . & \overline{\omega_n}(N) & \overline{\omega_n}(N)e_e(N) & \overline{\omega_n}(N)\Delta e_w(N) \end{bmatrix} \quad (35)$$

And Y is an X (1+ input variables x 1) x1=75 x1 vector unidentified consequent parameters as

$$k=[m_1 n_1 r_1, m_2 n_2 r_2 ....m_n n_n r_n]^T \quad (36)$$

In the above case, in training 10,000 input–output patterns are used which gives complexity, so the solution may not exist to the Eq. (40). As an alternative, least squared estimate of K should be identified to find out the exact solution with minimizing squared error as: $Ak-D_{1-N}^2$.

By using the pseudo-inverse technique, the least-squares estimate is achieved which is as follows

$$k^*=(A^T A)^{-1} A^T D_{1-m}.$$

where $(A^TA)^{-1} A^T$ is the pseudo inverse of A. After the establishment of consequent parameters, the error vector e and output vector D_1 can be calculated as $e=D_{1-N}-D_1$. A.

Backward Pass

The back-propagation algorithm is used in the backward pass. By using chain rule, the antecedent parameters are updated and error signals are propagated. The chain rule can be represented in equation form as

$$\Delta a=-\eta\frac{\partial E}{\partial a}=-\eta\frac{\partial E}{\partial e}x\frac{\partial e}{\partial D_1}x\frac{\partial D_1}{\partial(\overline{\omega_1}F_1)}x\frac{\partial(\overline{\omega_1}F_1)}{\partial\overline{\omega_1}}x$$
$$\frac{\partial\overline{\omega_1}}{\partial\omega_1}x\frac{\partial\omega_1}{\partial\omega A_1}x\frac{\partial\omega A_1}{\partial a} \quad (37)$$

Where η = learning rate

E = Squared error instantaneous value for the T2NF Controller

$$E=\frac{1}{2}e^2=\frac{1}{2}(D_{1-N}-D_1)$$

Where

$$\Delta a=-\eta(D_{1-m}-D_1)(-1)F_1\, x\frac{\overline{\omega}j(1-\omega_j)}{\omega_j}x\frac{\omega_j}{\omega_{A_j}}x\frac{\omega_{A_j}}{\partial a}$$

$$\frac{\partial\omega_{A_j}}{\partial a}=\frac{1}{\left[1+\left(\frac{e_w-a}{c}\right)^{2b}\right]^2}X\frac{1}{c^2 b}x\,2b\,x(e_w-a)^{2b-1}x(-1)$$

$$=\omega_{A_j}^2\, x\frac{2b}{c}\, x\left(\frac{e_w-a}{c}\right)^{2b-1}$$

Similarly, the parameters b and c can be determined by applying corrections.

VI. RESULTS AND DISCUSSION

The proposed Indirect Vector Control IMD with Multilevel inverter as shown in Figure.4. In this, currents commands i^*_{DS} and i^*_{QS} are compared with the respective i_{DS} and i_{QS}. The drive system shown in Figure 4. is modeled in MATLAB/Simulink.

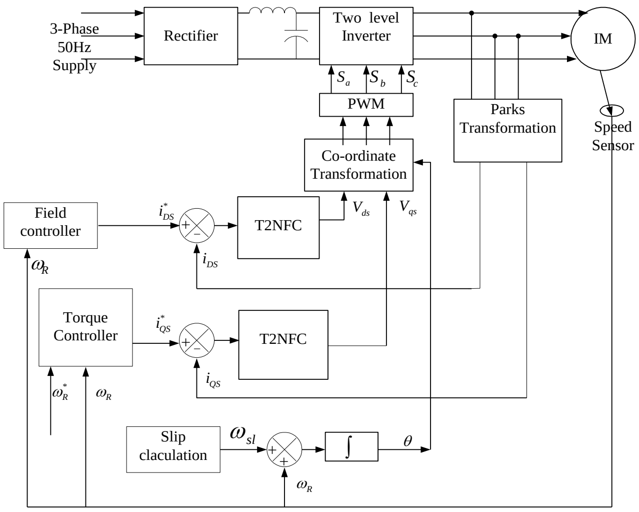

Figure 4. Indirect Vector Control Induction motor drive

During starting

The induction motor performance during starting is depicted in fig .5(a), 5(b) and 5(c). and it shows that maximum output current during the startup is reduced in comparison with conventional PI controlled system and type-I neuro fuzzy controller-based system. The maximum torque obtained with normal PI controlled system is about 12.2 N-m and type-I neuro fuzzy controller-based system is 13 N-m but with type 2 Neuro Fuzzy controller is 13.7 N-m. Due to this better speed is achieved.

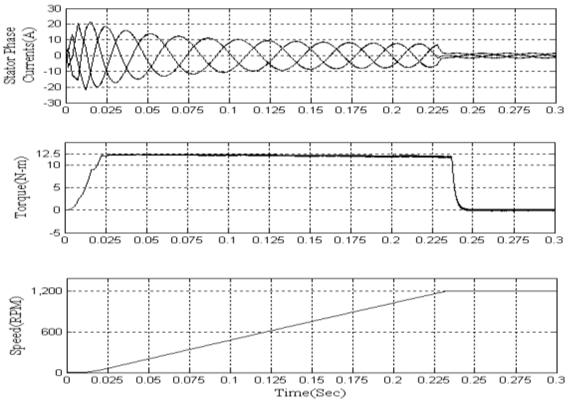

(a) PI controllers based indirect vector control

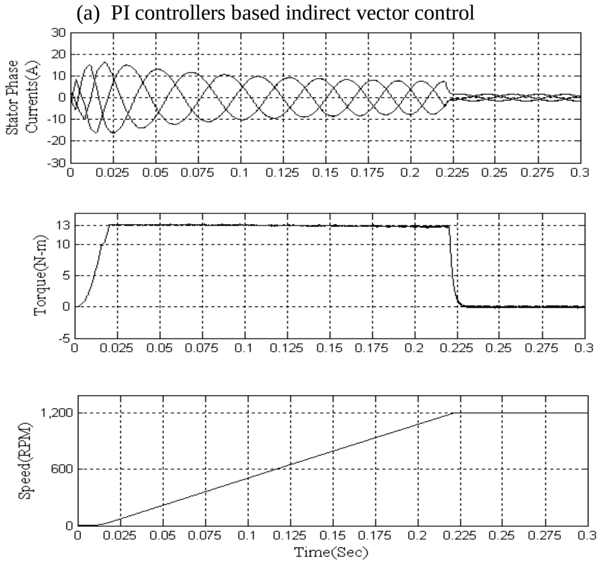

(b) Neuro Type-1 fuzzy controlled indirect vector control

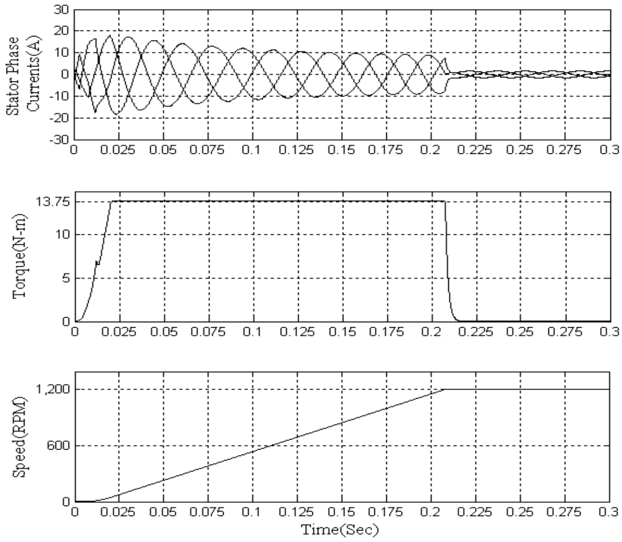

(c) Neuro Type-2 fuzzy controlled indirect vector control

Figure 5. Induction motor performance during starting up

B. Response during steady state

The induction motor performance during steady state as depicted in fig 6. (a), (b) and (c). By using Proportional integral controller, the torque ripple is between +0.35 to -0.35, with type 1 neuro fuzzy controller is between +0.2 to -0.2. and with neuro type 2 fuzzy controller is between +0.02 to -0.02. By using type 2 neuro fuzzy controller-based system the ripple content in the stator phase current, the speed response oscillations about reference speed 1200 RPM value is less as comparison with the PI controlled system and with neuro type 2 fuzzy controller-based system.

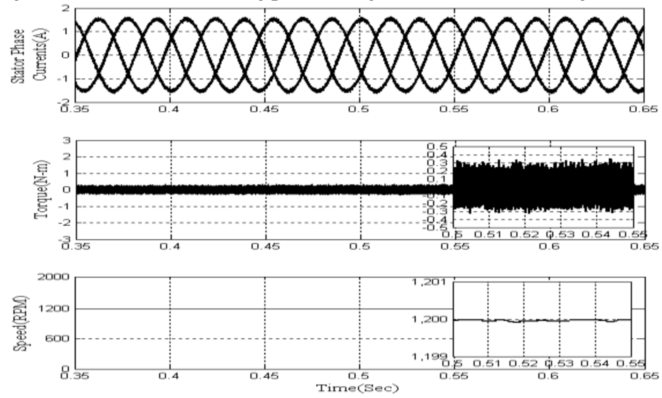

(a) PI controller based indirect vector control

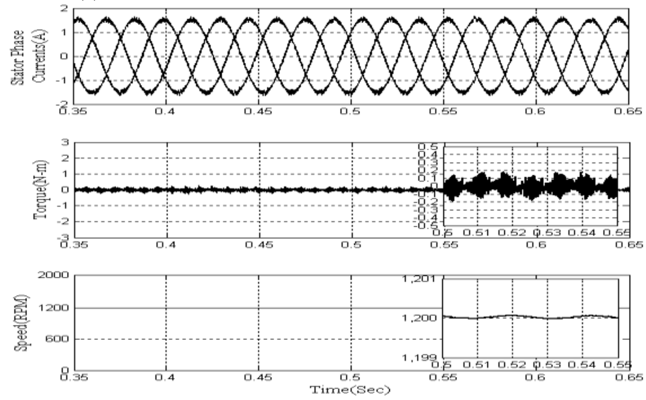

(b) Neuro Type-1 fuzzy controlled indirect vector control

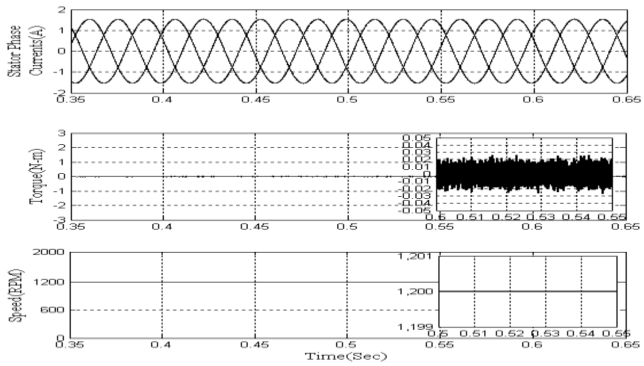

(c) Neuro Type-2 fuzzy controlled indirect vector control

Figure 6. Induction motor performance at steady state

C. Induction Motor response when Step change in load torque

The response when step change in load torque as depicted in fig 7. (a), (b) and (c). By using Neuro type 2 Fuzzy controller-based system the ripples in current waveforms and torque wave forms is reduced. The momentary speed decrease is also very less with Neuro type 2 Fuzzy controller-based system during the load change.

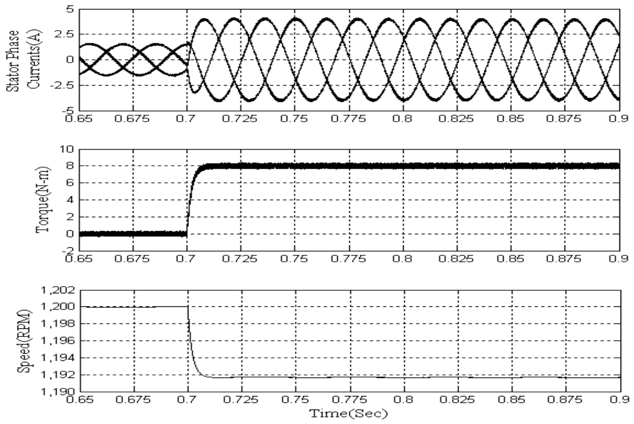

(a) PI controller based indirect vector control

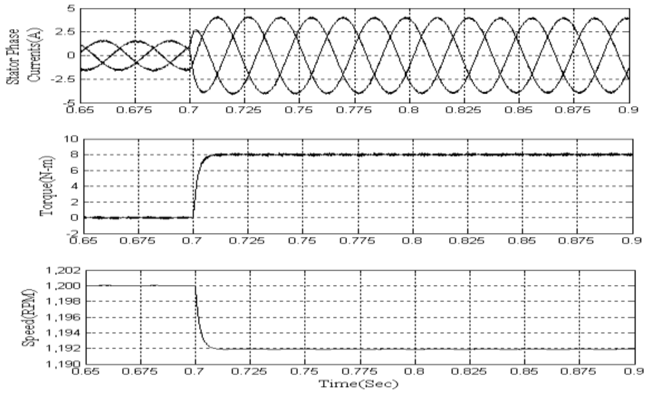

(b) Neuro Type-1 fuzzy controlled indirect vector control

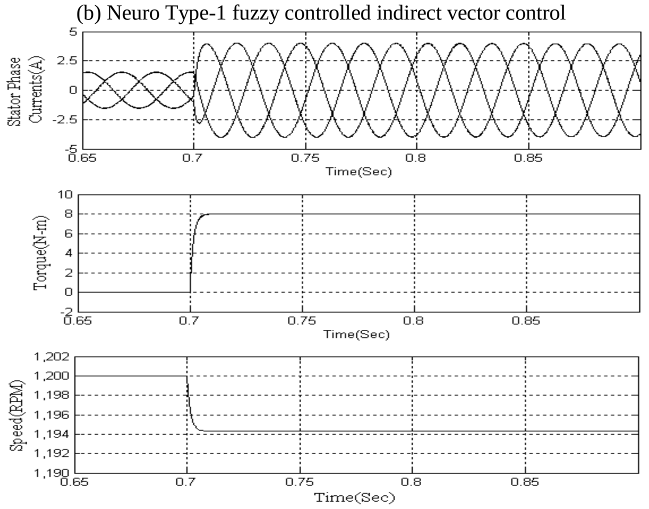

(c) Neuro Type-2 fuzzy controlled indirect vector control

Fig 7. Induction motor performance during step changing in load torque

VII. EXPERIMENTAL VALIDATION

The proposed neuro type 2 fuzzy controlled induction motor drive was validated and verified under various operating conditions in real time using a dSPACE RTI-1104 controller. The DSPACE graphical user interface (GUI) is used to monitor the inverter behavior and performance in the real time application.

The control process of the induction motor is designed in MATLAB/Simulink. To implement in real time the C code generates automatically by using MATLAB/Simulink with dSPACE. The modulator gets the error and change in error at the input and produces duty ratios at its output. By using type 2 neuro fuzzy control algorithm the data is generated to train the network and data is computed using the dSPACE.

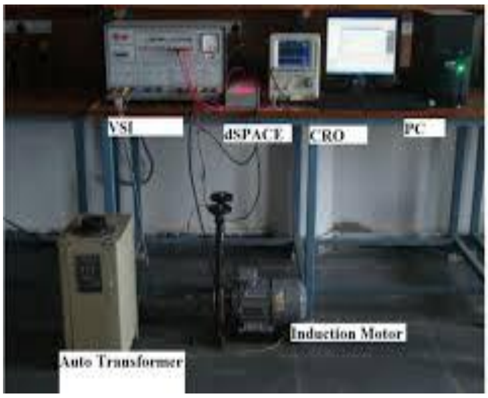

Figure 8. Experimental setup of Dspace-1104

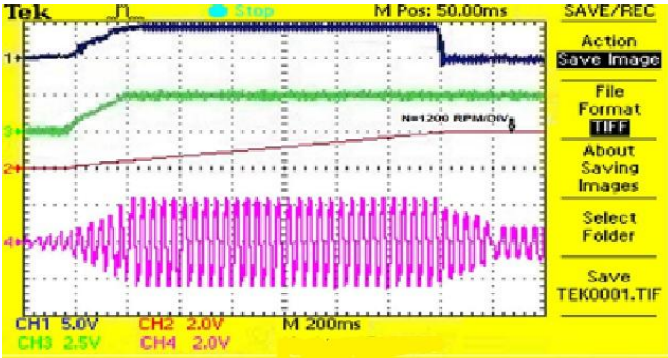

a. PI controller based indirect vector control

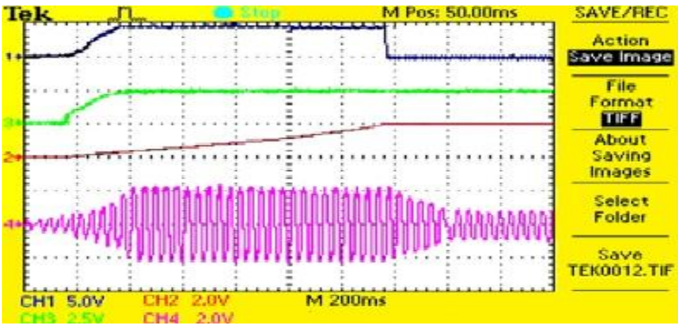

b. Neuro type-1 fuzzy based system

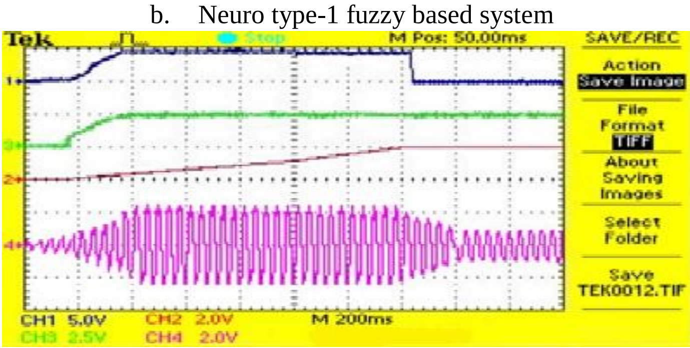

c. Neuro type-2 Neuro fuzzy based system

Fig 9. Induction motor performance during starting

During staring, the induction motor performance with PI, TINFC and T2NFC as sown in fig 9(a),9(b) and 9(c). Fig 9(a). With conventional PI controller the torque (The)12.5N-m of IM develops to overcome the inertia and picks up the motor speed (Nm) up to the reference value and it settles at 0.75s. The current also arises due to increasing the torque developed by the IM and it is settled at 0. 75s.

With T1NFC the torque of 13N-m of induction motor develops and motor speed settles at 0.65s which is shown in fig 9(b).Fig 9(c) shows that the torque 13.75N-m of induction motor develops and motor speed settles at 0.63s which is faster as compared to conventional PI and type 1 controllers.

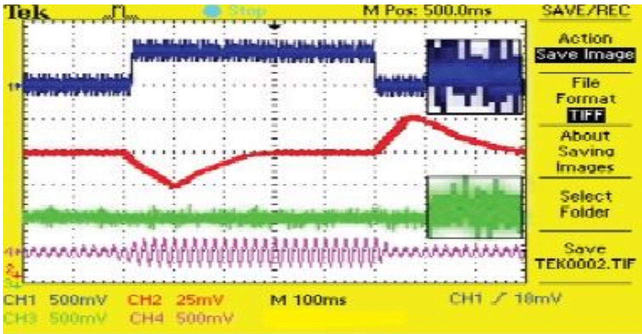

a. conventional PI Controller based system

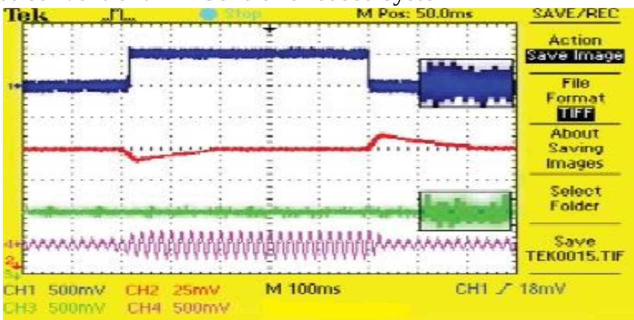

b. Type-1 Neuro fuzzy based system

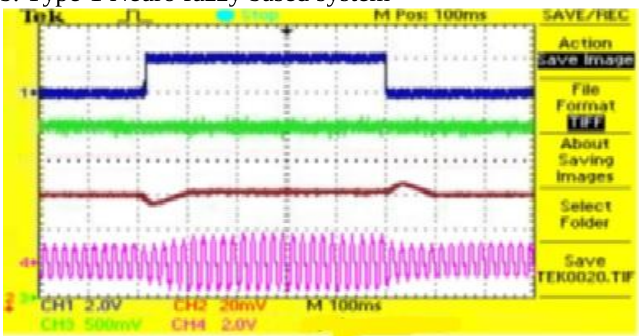

c.Type-2 Neuro fuzzy based system

Fig 10. Responses of an induction motor drive at steady state and step change in load torque

By using PI controller, it is observed that the torque (T_e) increases to 4 N·m and falls down to 0 N ·m because of the load changes. The torque ripple is in between +1.2 to -1.2. The induction motor speed decreases and increases to 1440 and 1460 rpm at the 0.2s and 0.7s instants and it settles at 0.5 and 1 s, respectively. Moreover, the current suddenly increases to 2.2 A at 0.23 s and again falls down to 1.5 A at 0.73 s due to increase and decrease in the load, respectively. But throughout the operation the flux is maintained constant as shown in fig 10 (a). By using TINFC the wave forms shown in fig 10 (b) seems to be same but there is drastic change in torque and flux distortion. The torque ripple is in between +0.9 to -0.9 N-m and speed fluctuations is also very less. Fig 10(c) shows the torque ripple is between +0.02 to -0.02. The flux is almost constant. It is also shows that the torque and current ripples are reduced with N2TFC as compared to type1 and conventional PI controller.

VIII. CONCLUSION

The performance parameters of induction motor such as current, torque and speed under various operating conditions is analyzed by simulation and also by experimental validation. The performance comparison is made using conventional PI controller, NT1FC and NT2FC.During the starting the maximum current is reduced, the torque is increased by 4% and required speed reached quickly by N2TFC compare to N1TFC and conventional PI Controller. During steady state condition it is observed that torque is reduced by 33% due to this oscillation in the speed response is less with N2TFCcompare to N1TFC and conventional PI Controller. It is also observed that the ripple content in the current wave form such as i_d and i_q which are fed to the current controller is also less. During the step changing the load torque the decrement in speed value is less with N2TFC compared to N1TFC and conventional PI Controller. The overall performance of induction motor under dynamic conditions is better with N2TFC and it is improved by 20 to 30% compare to N1TFC and conventional PI both with simulation and experimental validation.

REFERENCES

1. L.Harnefors,"Design and analysis of general rotor flux oriented vector control system," IEEE Transactions on Indusrial Electronics,vol.48,no.2,pp.383-390,2001.
2. A.M.Khambadkone and J.Holtz, "Vector controlled induction motor drive with a self commissioning," IEEE Transactions on Industrial Electronics,vol.38,no.5,pp.322-327,1991.
3. R.Krishanan,Electric Motor Drives:Modelling analysis and control vol.626:Prentics Hall Upper Saddle River,NJ,2001.
4. G.Gonzale Acevedo,G.M.N Vargas,J.J.C Torres and J.Jairo, "Design of Rotor Flux Oriented Vecor Control Systems for Induction Motor," International Power Electronics and Motion Control Conference, 2012,pp.1384-1388.
5. R.Arulmozhiyal,K.Baskaran and R.Manikandan, "A Fuzzy based PI speed controller for indirect vector controlled induction motor drive," India International Conference in Power Electronics,2010,pp.1-7 .
6. S.Rafa,A.Larabi,L.Barazane,M.Manceur,N.Essounbouli and A.Hamzaoui, "Fuzzy Vector control of induction motor," in ICNSC,2013,pp.815-820.
7. A.K.Gupta and A.M.Khambadkone, " A Space vector modulation scheme for Multilevel invereter based on two level space vector PWM," IEEE Transaction on Industrial Electronics,vol.53,pp.1631-1639,2006.
8. Durgasukumar,Jayachandranath Jitendranath and Suman Saranu, "Three-Level Inverter fed Induction Motor Drive Performance Improvement with Neuro Fuzzy Space vector Modulation," Electric Power Components and Systems,vol.42,no.15,pp.1633-1646,2014.
9. G.Durgasukumar and M.K.Pathak, "Comparison of Adaptive Neuro Fuzzy based Space Vector Modulation for Two-Level Inverter," International Journal of Electrical Power and Energy Systems,Elsevier,vol.38,no.1,pp.9-19,2012.
10. S.Krishnama Raju and G.N.Pillai, "Design andImplementation of Typr-2 Fuzzy Logic Controller for DFIG Based Wind Energy Systems in Distribution Networks," IEEE Transactions on sustainble energy,vol.7,no.1pp.345-353,2016.
11. Venkataramana Naik,Auroinda Panda and S.P Singh, "A Three Level Fuzzy-2 DTC of Induction Motor Drive Using SVPWM," IEEE Transactions on Industrial Electronics vol.63.no.3,pp.1467-1479,2016.
12. Venkataramana Naik,S.P.Singh and G.Durgasukumar, "An Improved performance of F2DTC induction motor using five level SVM," IEEE International Conferece on Power Electronics Drives and Energy Systems,2016,pp.1-6.

13. T.Ramesh,A.K.Panda and S.S.Kumar," Type-1 and Type-2 fuzzy logic spedd controller based high performance directtorque and flux controlled induction motor drive," in IEEE INDICON,2013,pp.1-6.
14. R.N.Mishra and K.B.Mohanthy, "Real time implementation of an ANFIS based induction motor drive via feedback linearization for performance enhancement," International Journal of Engineering Science and Technology,Elsevier,vol.19,no.4,pp.1714-1730,2016.
15. Rahib H,Abiyeva,Okyay Kanay,Tayseer Alshanaleha and Fakhreddin Mamedoya, " A type-2 neuro fuzzy system based on clustering and gradient techniquesapplied to system identification and channel equalization," International Journal of Applied soft computing,Elsevier,vol.11,no.1,pp.1396-1406,2011.
16. Saleh Masumpoor,Hamid yaghobi and Mojtaba Ahmadieh Khanesar, "Adaptive Sliding mode type-2 neuro fuzzy control of an induction motor," International Journal of Expert Systems with Applications,Elsevier,vol.42,no.19,pp.6635-6647,2015.
17. H.Sathish Kumar and S.S Parthasarathy, " A Novel neuro fuzzy controller for vector controlled induction motor drive," International Conference on Altrnative Energy in Developing Countries and Emerging Econamies,2017,pp.698-703.
18. A.K.Das,K.Subramanian and S.Suresh, "An Evolving Interval Type-2 Neuro-Fuzzy Inference sytems and its Meta cognitive Sequential Learning Algorithm," IEEE Transaction on Fuzzy Systems,vol.23,no.6,pp.2080-2093,2015.
19. T.Abhiram and M.K.Pathak G.Durgasukumar "Type-2 fuzzy based SVM for Two-level inverter fed induction motor drive," IEEE-IICPE Delhi, 2012 pp.1-6.
20. B Pakkiraiah, G Durga Sukumar "Enhanced performance of an asynchronous motor drive with a new modified adaptive neuro-fuzzy inference system-based MPPT controller in interfacing with dSPACE DS-1104," International Journal of Fuzzy Systems, Springer vol.19,no.6,pp.950-1965,2017.
21. G.Durgasukumar and M.K. Pathak "Nuero-Fuzzy based Torque Ripple Reduction and Performance Improvement of VSI fed Induction Motor Drive," International Journal of Bio Inspired Computation, InderScience,vol.4.no.2,pp.63-72,2012.

AUTHORS PROFILE

R.Ramanjan Prasad received B. Tech degree in Electrical and Electronics Engineering, in 2005 and M. Tech degree in Power Electronics in 2009. He is presently pursuing Ph. D from Vignan's Foundation for Science Technology and Research University in the department of Electrical and Electronics Engineering, with the specialization of Power Electronics and drives. His research interests are in power electronics and drives, neural networks and fuzzy logics and new research eras in renewable energy sources.

G. Durga Sukumar received bachelor and master degrees in Electrical Engineering from J.N.T.U, Hyderabad (India) and completed his Ph. D degree in the Electrical Engineering Dept, Indian Institute of Technology, Roorkee, India. His research interests include power electronics and electric drives, machines and new research eras in solar energy incorporated with type 2 / neuro fuzzy- based controllers